Complex Planetary Systems II: Latest Methods for an Interdisciplinary Approach
Proceedings IAU Symposium No. 382, 2024
A. Lemaitre & A.-S. Libert, eds.
doi:10.1017/S174392132300399X

Transversal Yarkovsky acceleration for Apophis through jet transport

Luis Benet[1] **and Jorge A. Pérez Hernández**[2]

[1]Instituto de Ciencias Físicas, Universidad Nacional Autónoma de México (UNAM)
Av. Universidad s/n, Col. Chamilpa, 62210 Cuernavaca, México
email: benet@icf.unam.mx

[2]Telespazio Germany GmbH, Darmstadt, Germany
email: perez.hz@gmail.com

Abstract. In this contribution we describe the jet transport techniques that we used in Pérez-Hernández and Benet (2022) for the estimation of the Yarkovsky transversal acceleration for (99942) Apophis, which included optical and radar astrometry observations obtained during 2021 Apophis' fly-by. Our numerical approach exploits automatic differentiation techniques which improve the orbital determination problem. We obtain a non-zero Yarkovsky parameter $A_2 = (-2.899 \pm 0.025) \times 10^{-14}$ au d^{-2} which is consistent with other recent determinations of this parameter. Our results allow to constrain the collision probabilities for the close approaches in 2029, 2036 and 2068.

Keywords. Yarkovsky effect, Apophis, Jet transport

1. Introduction

Accurate predictions of the orbital motion of asteroid (99942) Apophis are driven by the Yarkovsky effect (Giorgini et al. 2002; Chesley 2006). This is a non-gravitational acceleration arising from the anisotropic thermal re-emission of absorbed radiation (Vokrouhlický et al. 2000; Bottke Jr et al. 2006). Since the main dynamical manifestation of the Yarkovsky effect is a drift in the semimajor axis, this acceleration can be modeled as $\dot{\vec{v}}_a = A_2\, g(r_{a,S})\hat{t}_{a,S}$, where $r_{a,S}$ is the radial distance from the Sun to the asteroid, and $\hat{t}_{a,S}$ represents the transversal unit vector along the motion (Farnocchia et al. 2013). The function $g(r)$ describes the dependence on the solar distance, and it is often modelled as $g(r) = (r_0/r)^2$ with $r_0 = 1$ au. The parameter A_2 corresponds to a transversal, non-conservative Yarkovsky acceleration, which is obtained during the orbit determination process. Early attempts to determine A_2 for Apophis resulted in values whose uncertainty could not rule out a pure gravitational interaction; see e.g. Vokrouhlický et al. (2015); Brozović et al. (2018); Del Vigna et al. (2018); Greenberg et al. (2020). Apophis is of interest because, while a collision with Earth has been ruled out for its next close approach in April 13th 2029, more high-quality observations are required to rule out collisions for later close approaches, in particular in 2036 and 2068.

In this contribution, we provide details about the techniques, known as jet transport, which we used to determine the value of A_2 and its uncertainty Pérez-Hernández and Benet 2022, exploiting most optical and radar observations publically available, including observations made during the last close encounter in 2021.

2. Orbit determination

We briefly describe the orbit determination problem, following Milani and Gronchi (2010). First, in order to determine the orbit of the asteroid, a precise dynamical model is required. This is essentially a system of differential equations which includes all important interactions, as well as the initial conditions $\tilde{\mathbf{x}}_0$ for the asteroid defined at a given epoch t_0. The goal is to obtain the nominal orbital elements $\mathbf{x}_0$, together with other unknown parameters of the dynamical model such as A_2, which is the best fit to the observations. The observational quantities are written as $r_k \pm \sigma_k$, where the index k labels the observation, and also refers to the time t_k when the observation was obtained. Here, r_k can be the right ascension and the declination for optical astrometry, or the time delay or the Doppler shift for radar observations. The associated observational uncertainty is σ_k.

In order to link the observations with the variables which are computed from the dynamical model, $\mathbf{x}(t)$, we require the observation function $R(\mathbf{x}(t_k), t_k)$ for each different observed quantity, which depends indirectly on the initial condition $\tilde{\mathbf{x}}_0$. The observation function R is used to construct the observed-minus-computed (O-C) residuals, $\xi_k = r_k - R(\mathbf{x}(t_k), t_k)$, which provide a description of the quality of the dynamical model.

In order to obtain the nominal orbital elements, we introduce the mean-squared residual function

$$Q(\tilde{\mathbf{x}}_0) = \frac{1}{m}\sum_{k=1}^{m}\frac{\xi_k^2}{\sigma_k^2} = \frac{1}{m}\xi^T\mathbf{W}\xi, \tag{1}$$

where m denotes the number of observations, and $\mathbf{W}$ is the diagonal matrix with the inverse squared observational uncertainties. The nominal orbital elements, which we shall denote as $\mathbf{x}_0$, correspond to the minimum of $Q(\tilde{\mathbf{x}}_0)$. The orbit determination problem can thus be interpreted as an optimization problem, with the mean-squared residual function Q as the target function. We note that any (constant) parameters to be determined, such as A_2, can be included as dynamical variables in $\mathbf{x}$, adding new equations of motion to the dynamical model for the NEA, i.e., $\dot{A}_2 = 0$.

2.1. *Differential correction approach*

In order to find the minimum $\mathbf{x}_0$ of the target function, $Q(\tilde{\mathbf{x}}_0)$ is Taylor-expanded around the unknown nominal orbit, up to second order in the deviations with respect to $\mathbf{x}_0$; we note that third- and higher-order corrections are disregarded. Imposing $\frac{\partial Q}{\partial \mathbf{x}_0}(\mathbf{x}_0) = 0$ at the nominal orbit, and using a first guess for the nominal orbit $\mathbf{x}_0^*$, which is assumed to be close enough to $\mathbf{x}_0$, the optimization problem is solved from the (truncated) Taylor expansion for $Q(\tilde{\mathbf{x}}_0)$ by a Newton-like iteration method as

$$\mathbf{x}_{j+1}^* = \mathbf{x}_j^* - \Gamma\frac{\partial Q}{\partial \mathbf{x}_0}(\mathbf{x}_j^*). \tag{2}$$

Here, $\mathbf{x}_j^*$ is the j-th iterate of the Newton method and $\Gamma = \left(\frac{\partial^2 Q}{\partial \mathbf{x}_0^2}\right)^{-1}$, which is evaluated at $\mathbf{x}_j^*$, is the covariance matrix. Denoting by $\mathbf{B} = \frac{\partial \xi}{\partial \mathbf{x}_0}(\mathbf{x}_j^*)$ the derivative of the O-C residuals with respect to the nominal solution, also known as the design matrix, and by $\mathbf{H} = \frac{\partial^2 \xi}{\partial \mathbf{x}_0^2}$ the Hessian, from Eq. (1) we have

$$\frac{\partial Q}{\partial \mathbf{x}_0} = \frac{2}{m}\xi^{\mathbf{T}}\mathbf{W}\mathbf{B}, \tag{3}$$

$$\frac{\partial^2 Q}{\partial \mathbf{x}_0^2} = \frac{2}{m}\left(\mathbf{B}^T\mathbf{W}\mathbf{B} + \xi^T\mathbf{W}\mathbf{H}\right). \tag{4}$$

These quantities are used in (2) to obtain an approximation of the nominal solution.

https://doi.org/10.1017/S174392132300399X Published online by Cambridge University Press

The design matrix is constructed by solving the first variational equations associated to the dynamical model. Denoting by N the dimensionality of $\mathbf{x}(t)$ including any model parameters, there are N first-order equations of motion associated to the dynamical model, and N^2 for the first variational equations. The three-index Hessian is clearly even more expensive to determine in terms of the number of differential equations to be solved, and it is often neglected. The variant of Newton's method that neglects the higher order corrections in $(\mathbf{x}_k^* - \mathbf{x}_0)$ of $Q(\mathbf{x}_k^*)$ and disregards the Hessian is known as the differential corrections' method (Milani and Gronchi 2010).

2.2. *Jet transport*

Jet transport is a technique used to solve initial value problems which, by exploiting automatic differentiation, allows obtaining insight into the dynamics in the neighborhood of the initial condition. Instead of solving the initial value problem for a specific initial condition $\tilde{\mathbf{x}}_0$, the equations of motion are solved for $\tilde{\mathbf{x}}_0 + \underline{\boldsymbol{\delta}}$, where the *symbol* $\underline{\boldsymbol{\delta}}$ denotes the deviations from the initial condition $\tilde{\mathbf{x}}_0$, which are assumed to be small enough. Jet transport only requires that the specific integration solver used for the differential equations works with a polynomial manipulator.

The solutions of the differential equations at time t are then truncated polynomials in $\underline{\boldsymbol{\delta}}$ around the initial condition, which we write as

$$\mathbf{x}(t, \underline{\boldsymbol{\delta}}) \simeq \mathbf{x}^{[0]}(t) + \mathbf{x}^{[1]}(\underline{\boldsymbol{\delta}})(t) + \mathbf{x}^{[2]}(\underline{\boldsymbol{\delta}}^2)(t) + \cdots + \mathbf{x}^{[q]}(\underline{\boldsymbol{\delta}}^q)(t). \tag{5}$$

Here, the zero-order solution in $\underline{\boldsymbol{\delta}}$, $\mathbf{x}^{[0]}(t)$, is just the solution at time t for the initial condition $\tilde{\mathbf{x}}_0$. In turn, $\mathbf{x}^{[k]}(\underline{\boldsymbol{\delta}}^k)(t)$ represents the k-order correction at time t in $\underline{\boldsymbol{\delta}}$. This k-order correction is a homogeneous polynomial in $\underline{\boldsymbol{\delta}}$ of degree k, which we have emphasized by using the notation $\underline{\boldsymbol{\delta}}^k$; it includes the contribution of all monomials of degree k in the independent deviations of $\underline{\boldsymbol{\delta}}$. It can be shown that the q-order solution given by Eq. (5) is a solution of the variational equations of order less or equal to q (Gimeno et al. 2023). Then, jet transport techniques allow including higher order approximations of the target function $Q(\tilde{\mathbf{x}}_0)$, and consequently a better approximation of the nominal orbital elements.

From the jet-transport solution (5) at the epochs of the observations t_k, we have the O-C residuals as truncated polynomials up to degree q. From them, we can compute the expansion, up to degree q in the deviations $\underline{\boldsymbol{\delta}}$, of the mean square residual function (1), which we thus write as

$$Q(\underline{\boldsymbol{\delta}}) \simeq Q^{[0]} + Q^{[1]}(\underline{\boldsymbol{\delta}}) + Q^{[2]}(\underline{\boldsymbol{\delta}}^2) + \cdots + Q^{[q]}(\underline{\boldsymbol{\delta}}^q). \tag{6}$$

The minimization problem for the nominal orbit can be stated as above. The subtle difference is that Eq. (6) permits implementing Newton's method (2) directly, since all needed derivatives with respect to $\mathbf{x}_0$ can be computed directly from the polynomial expansion (6), and $Q(\underline{\boldsymbol{\delta}})$ includes all contributions up to order q in the target function. Aside from obtaining the nominal solution $\mathbf{x}_0$, the correlation matrix Γ can also be computed directly from its definition.

3. Results for Apophis

In this section we briefly describe the dynamical model and the results for Apophis; further details can be found in Pérez-Hernández and Benet (2022). We have produced our own planetary ephemeris (Pérez-Hernández et al. 2021), integrating a model essentially equivalent to JPL DE430 (Folkner et al. 2014). The dynamical model for Apophis includes

https://doi.org/10.1017/S174392132300399X Published online by Cambridge University Press

Table 1. International Celestial Reference Frame barycentric initial conditions (position, velocity and nominal Yarkovsky parameter) for the gravity-only (OR6) and non-gravitational (OR7) solutions. The epoch is December 17, 2020 00:00:00.0 (TDB). The symbols x_0, y_0, z_0 represent initial positions in au, and v_{x0}, v_{y0}, v_{z0} represent initial velocities in au/d. A_2 is the Yarkovsky transversal parameter in au/d^2, multiplied by 10^{14}. Numbers in parentheses represent the order of magnitude of the formal 1-sigma uncertainty.

Init. cond./sol.	OR6	OR7
x_0 [au]	$-0.18034816(472) \pm 7.05 \times 10^{-9}$	$-0.18034828(526) \pm 7.12 \times 10^{-9}$
y_0 [au]	$0.94069116(764) \pm 1.71 \times 10^{-9}$	$0.94069105(951) \pm 1.94 \times 10^{-9}$
z_0 [au]	$0.34573641(385) \pm 4.03 \times 10^{-9}$	$0.34573599(029) \pm 5.41 \times 10^{-9}$
v_{x0} [au/d]	$-0.0162659357(312) \pm 3.31 \times 10^{-11}$	$-0.0162659397(882) \pm 4.79 \times 10^{-11}$
v_{y0} [au/d]	$4.39163(792) \times 10^{-5} \pm 6.68 \times 10^{-11}$	$4.39154(800) \times 10^{-5} \pm 6.72 \times 10^{-11}$
v_{z0} [au/d]	$-0.000395210(949) \pm 1.24 \times 10^{-10}$	$-0.000395204(013) \pm 1.38 \times 10^{-10}$
A_2 [$\times 10^{14}$ au/d^2]	0.0 (fixed)	$-2.8(988) \pm 2.48 \times 10^{-2}$

the Sun, all planets, the Moon and Pluto, 16 main-belt asteroids, post-Newtonian corrections (except for the asteroids), corrections due to J_2 for the Earth, and the transversal Yarkovsky effect A_2; the code is publically available (Pérez-Hernández et al. 2021). The integration of the differential equations has been performed using Taylor's method of degree 25 with an absolute tolerance 10^{-30}.

Jet transport is applied up to degree $q = 5$, and we have produced two best-fit solutions corresponding to slightly different dynamical models of Apophis: First, a purely gravitational model which does not include the Yarkovsky effect ($A_2 = 0$), and thus jet transport is applied using 6 variables; this solution is denoted as OR6 below. Second, the same model now including A_2; in this case jet transport is applied for 7 degrees of freedom, and the corresponding solution is referred as OR7. For the initial guess, we used JPL's #197 gravity-only solution at the epoch December 17, 2020 00:00:00.0 (TDB) epoch (Brozović et al. 2018). The nominal initial conditions obtained for each model are given in Table 1, using the same epoch indicated above. Notice that the quotient of the nominal value of A_2 obtained in OR7, divided by the formal uncertainty of the same parameter, i.e., the signal-to-noise ratio for A_2, is $\mathrm{SNR}_{A_2} \approx 117$, implying a non-zero value.

In Fig. 1 we present the optical astrometry O-C residuals and in Fig. 2 the O-C residuals for the radar observations, obtained from the best orbital fit for the gravity-only model (OR6) with purple symbols, and for the model including non-gravitational interactions (OR7) with green symbols. We note that the distributions of the projected optical O-C residuals for the OR6 solution, plotted in the side and upper panels of Fig. 1, are bimodal distributions, whereas the OR7 solution yields single bump distributions; the latter are closer to Gaussian distributions, which we expect from the central limit theorem, under the assumption of uncorrelated observations. We also remark that the uncertainties associated to the O-C radar residuals of the OR7 solution in Fig. 2 are all consistent with zero. In more quantitative terms, the normalized root-mean-square error for the combined optical and radar fits is 0.979 and 0.306, respectively for the OR6 and OR7 solutions. Other quantities comparing the quality of the fit provided by each solution appear in Table 1 of Pérez-Hernández and Benet (2022); they show consistently better fit properties for the non-gravitational model OR7. From these observations we conclude that the OR7 solution better describes the combined optical and radar astrometry observations, and that the fit obtained by this solution yields a non-zero transversal Yarkovsky parameter.

Using the OR7 solution, Apophis orbit can be propagated forward in time to analyze the collision probability for the next close encounter in April 13th 2029, as well as in 2036 and 2068. We obtain vanishingly small values of the collision probabilities in all those close approaches (Pérez-Hernández and Benet 2022).

https://doi.org/10.1017/S174392132300399X Published online by Cambridge University Press

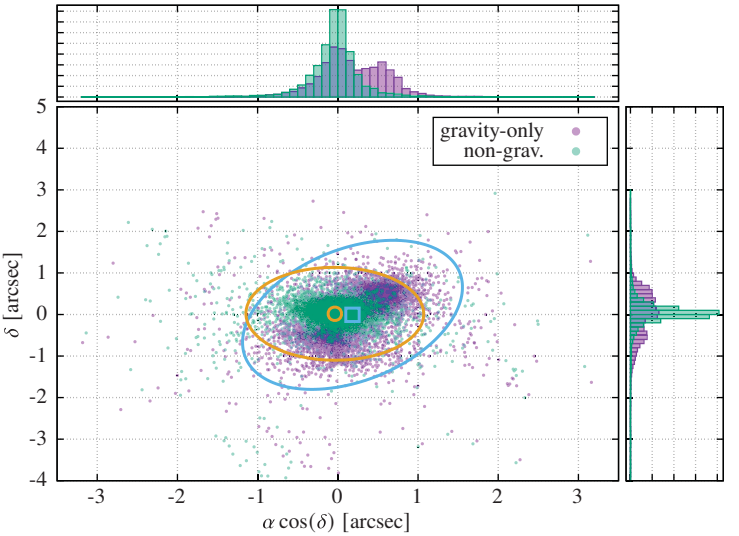

Figure 1. Optical astrometry O-C residuals for the OR6 (purple symbols) and OR7 (green symbols) orbital fits. The x-axis displays the right-ascension residuals, and the y-axis those for the declination. In the top and side panels, the distributions of these residuals are displayed for OR6 and OR7 solutions: for OR6 (in purple) notice that both distributions are bi-modal.

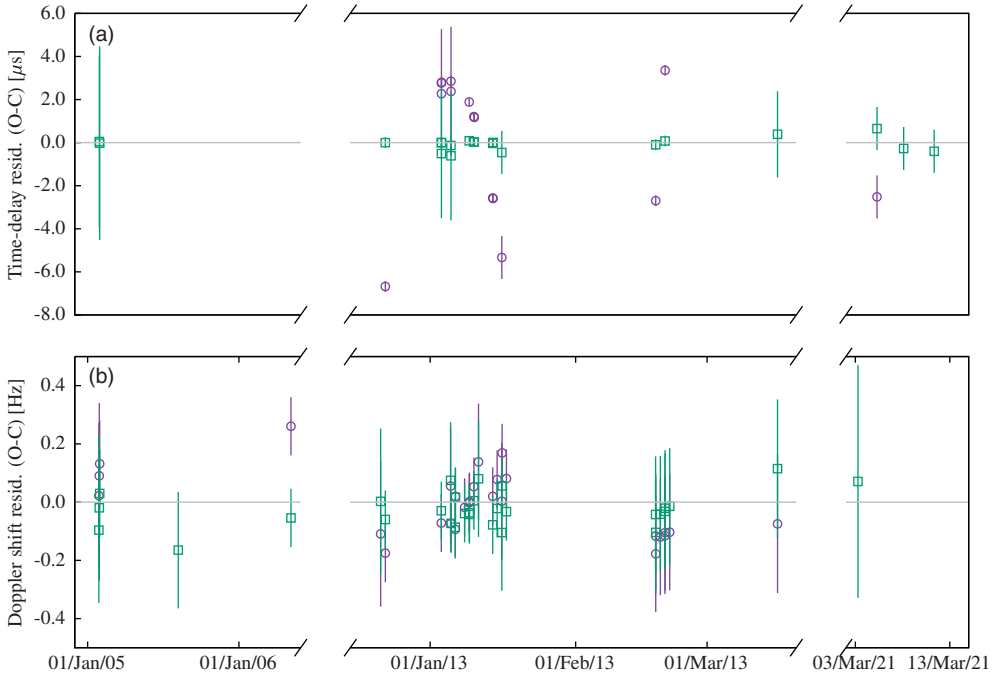

Figure 2. Radar astrometry O-C residuals in time, displaying separately the time delays and the Doppler shifts, for the OR6 (purple symbols) and OR7 (green symbols) orbital fits. We notice that all residuals of the OR7 solution, taking into account the observational error bars, are compatible with zero.

https://doi.org/10.1017/S174392132300399X Published online by Cambridge University Press

4. Summary and conclusions

In this contribution we have provided further details of our approach using jet transport to determine the transversal Yarkovsky parameter for Apophis. Using jet transport techniques we obtain semi-numeric high-order approximations of the target function, whose minimum we find through a Newton iteration method. Having such a high-order approximation of the target function allows us to compute directly the covariance matrix. With this scheme we obtained two nominal solutions compatible with all public available optical and radar astrometry: a purely gravitational model, the OR6 solution, and a model that incorporates the transversal Yarkovsky acceleration, the OR7 solution. Comparing both solutions, the one that yields a better fit is OR7, and the associated 1-sigma uncertainty associated with A_2 yields conclusively a non-zero value.

The OR7 value obtained for the transversal Yarkovsky parameter is $A_2 = -(2.899 \pm 0.025) \times 10^{-14}$ au d^{-2}, which yields a non-gravitational semi-major axis drift of $\langle \dot{a} \rangle = (-199.0 \pm 1.5)$ m yr^{-1}. This value of A_2 is consistent with the current value reported at JPLs small-body database for Apophis ssd, namely $A_2^{\rm JPL} = -(2.901 \pm 0.019) \times 10^{-14}$ au d^{-2}. In addition, it is also consistent with the value obtained by combining five very accurate stellar occultations by Apophis with the optical and radar astrometry observations by Souami et al. (2023) and Desmars et al. (2023), who obtained $A_2^{\rm occ} = -(2.8992 \pm 0.0161) \times 10^{-14}$ au d^{-2}. The consistency of these values, in particular with the last one, shows the efficiency of jet transport methods in the orbit determination problem.

Acknowledgments: We acknowledge financial support from the PAPIIT-UNAM project IG101122, and computer time provided through the project LANCAD-UNAM-DGTIC-284. We thank Bruno Sicardi for bringing to our attention the results obtained by Souami et al. (2023) and Desmars et al. (2023) through stellar occultations.

References

JPL Small-Body Database (data for Apophis). Accessed: 2023-08-23.

Bottke Jr, W. F., Vokrouhlickỳ, D., Rubincam, D. P., & Nesvornỳ, D. 2006, The Yarkovsky and YORP effects: Implications for asteroid dynamics. *ARAA*, 34, 157–191.

Brozović, M., Benner, L., McMichael, J., Giorgini, J., Pravec, P., Scheirich, P., Magri, C., Busch, M., Jao, J., Lee, C., *et al.* 2018, Goldstone and Arecibo radar observations of (99942) Apophis in 2012–2013. *Icarus*, 300, 115–128.

Chesley, S. R. Potential impact detection for Near-Earth asteroids: the case of 99942 Apophis (2004 MN 4). In Lazzaro, D., Ferraz-Mello, S., & Fernández, J. A., (eds.), *Asteroids, Comets, Meteors,* Proc. IAU Symposium No. 229, 2006, pp. 215–228.

Del Vigna, A., Faggioli, L., Milani, A., Spoto, F., Farnocchia, D., & Carry, B. 2018, Detecting the Yarkovsky effect among near-Earth asteroids from astrometric data. *A & A*, 617, A61.

Desmars, J., Souami, D., Vavilov, D., Hsu, H. M., De Pater, I., & Hestroffer, D. Apophis orbit with stellar occultations. In *Asteroids, Comets, Meteors Conference*, 2023, Abstract #2376, Houston. Lunar and Planetary Institute.

Farnocchia, D., Chesley, S., Vokrouhlický, D., Milani, A., Spoto, F., & Bottke, W. 2013, Near Earth asteroids with measurable Yarkovsky effect. *Icarus*, 224(1), 1–13.

Folkner, W., Williams, J., Boggs, D., Park, R., & Kuchynka, P. 2014, The planetary and lunar ephemerides DE430 and DE431. *Interplanet. Netw. Prog. Rep*, 196, 1–81.

Gimeno, J., Jorba, À., Jorba-Cuscó, M., Miguel, N., & Zou, M. 2023, Numerical integration of high-order variational equations of ODEs. *App Maths Comp*, 442, 127743.

Giorgini, J., Ostro, S., Benner, L., Chodas, P., Chesley, S., Hudson, R., Nolan, M., Klemola, A., Standish, E., Jurgens, R., *et al.* 2002, Asteroid 1950 DA's encounter with Earth in 2880: Physical limits of collision probability prediction. *Science*, 296(5565), 132–136.

Greenberg, A. H., Margot, J.-L., Verma, A. K., Taylor, P. A., & Hodge, S. E. 2020, Yarkovsky drift detections for 247 near-Earth asteroids. *AJ*, 159(3), 92.

Milani, A. & Gronchi, G. 2010,. *Theory of orbit determination*. Cambridge University Press.

Pérez-Hernández, J. A. & Benet, L. 2022, Non-zero Yarkovsky acceleration for near-Earth asteroid (99942) Apophis. *Comm Earth & Environm*, 3(1).

Pérez-Hernández, J. A. Ramírez-Montoya, L. E., & Benet, L. 2021,. NEOs.jl: Jet Transport-based Near-Earth Object orbital propagator and fitter in Julia. https://github.com/PerezHz/NEOs.jl.

Pérez-Hernández, J. A., Ramírez-Montoya, L. E., & Benet, L. 2021,. PlanetaryEphemeris.jl: A planetary and lunar ephemerides integrator based on JPL DE430 dynamical model. https://github.com/PerezHz/PlanetaryEphemeris.jl.

Souami, D., Desmars, J., Tanga, P., Tsiganis, K., de Pater, I., Hsu, Y. M., Ferreira, J., Siakas, A., Chesley, S., Dunham, D., Venable, R., Irwin, J., Watanabe, H., Bouquillon, S., Herald, D., & Preston, S. Stellar occultations by sub-km sized near Earth asteroids: Apophis and Didymos. In *Asteroids, Comets, Meteors Conference* 2023,, Abstract #2099, Houston. Lunar and Planetary Institute.

Vokrouhlický, D., Farnocchia, D., Čapek, D., Chesley, S., P.Pravec, P.Scheirich, & Müller, T. 2015, The Yarkovsky effect for 99942 Apophis. *Icarus*, 252, 277–283.

Vokrouhlický, D., Milani, A., & Chesley, S. 2000, Yarkovsky effect on small near-Earth asteroids: Mathematical formulation and examples. *Icarus*, 148(1), 118–138.

https://doi.org/10.1017/S174392132300399X Published online by Cambridge University Press